



Universidad
Carlos III de Madrid



This is a postprint version of the following published document:

Madrid, J. M., Pozuelo, J., Mendicuti, F. & Mattice, W. L. (1997): Molecular Mechanics Study of the Inclusion Complexes of 2-Methyl Naphthoate with α - and β -Cyclodextrins. *Journal of Colloid and Interface Science*, 193 (1), pp.: 112-120.

DOI: [10.1006/jcis.1997.5061](https://doi.org/10.1006/jcis.1997.5061)

© Elsevier, 1997



This work is licensed under a Creative Commons Attribution-NonCommercial-NoDerivatives 4.0 International License.

Molecular Mechanics Study of the Inclusion Complexes of 2-Methyl Naphthoate with α - and β -Cyclodextrins

Jose Manuel Madrid,* Javier Pozuelo,* Francisco Mendicuti,* and Wayne L. Mattice^{1,†}

*Departamento de Química Física, Universidad de Alcalá, 28871 Alcalá de Henares, Madrid, Spain;

and †Institute of Polymer Science, University of Akron, Akron, Ohio 44325-3909

Molecular mechanics calculations were employed to study the inclusion of 2-methyl naphthoate in α - and β -cyclodextrin *in vacuo* and in the presence of water as a solvent. The driving forces for complexation are dominated by nonbonded van der Waals host:guest interactions in both environments. The 2-methyl naphthoate penetrates completely into the cavity of β -cyclodextrin, but there is only partial penetration by the same molecule into the smaller cavity of α -cyclodextrin. © 1997 Academic Press

Key Words: cyclodextrins; inclusion complexes.

INTRODUCTION

Cyclodextrins (CDs) are toroid-shaped cyclic oligosaccharides composed of six (α -CD), seven (β -CD), eight (γ -CD), or more D-(α)-glucopyranose units joined by α -(1,4) linkages. These cyclic oligosaccharides have attracted attention because they spontaneously form inclusion complexes with a variety of guest molecules in aqueous media, since the internal cavity of the CD is more hydrophobic than the aqueous environment (1–3). Several experiments have been used to obtain the structural and thermodynamic parameters associated with the formation of the CD:guest inclusion complex (1–4). Among these methods are UV–visible absorption (5–9), nuclear magnetic resonance (10), circular dichroism (11, 12), potentiometry (13, 14), polarography (15, 16), liquid chromatography (17–20), fluorescence spectroscopy (6, 12, 21–25), X-ray crystallography (26), and electron spin resonance (ESR) spectroscopy (27, 28).

Complexation processes in solution depend on the size, shape, and hydrophobicity of the guest molecule. The driving forces that have been proposed include van der Waals interactions between guest and host, hydrogen bonding between the guest and the hydroxyl groups of the CD, release of strain energy in the macromolecular ring of the CD, and dipole–dipole and/or electronic charge interactions (1–3).

Molecular mechanics (MM) (29–31) and molecular dynamics (MD) (32–36) calculations have been performed in computational studies of the molecular structures and conformations of CDs in isolation, solvated by water, and in their crystalline forms. The application of these computational techniques to CD:guest inclusion compounds for a better understanding of the complexation process itself, however, has been more limited. Earlier MM works are from Harata (37) and Tabushi *et al.* (38). More recently, MM studies that use mainly MM2, MM3, and AMBER force field have been performed by Menger and Sherrod (39), Venanzani *et al.* (40), Ohashi *et al.* (41), Jaime and co-workers (42–46), Lipkowitz *et al.* (47), and Berg *et al.* (48). Ivanov and Jaime have also attempted MD studies of CD in the presence of water as a solvent (46).

Recently inclusion complexes of 2-methyl naphthoate (MN) with α -CD and β -CD were studied by steady-state fluorescence (49). The stoichiometry and formation constants were obtained from the ratio of the emission intensities for two bands of MN that are sensitive to the polarity of the medium. One-to-one stoichiometry was obtained for MN: α -CD and MN: β -CD complexes, but the equilibrium constants for formation at 25°C differ by an order of magnitude, being 200 ± 20 and $1965 \pm 160 \text{ M}^{-1}$, respectively. The experiments showed that the formation of MN: β -CD is accompanied by a more negative enthalpy change, ΔH , than the formation of MN: α -CD. The change in entropy, ΔS , was obviously important in determining the stability of both complexes. The formation of the MN: β -CD complex was accompanied by a large negative ΔS , but the entropy increased on formation of the MN: α -CD complex. Anisotropy measurements were used to interpret the different signs of ΔS . Two possible contributing factors are (1) α -CD insulates MN from the solvent better than does β -CD, and (2) MN may have more rotational freedom inside the larger cavity of β -CD, as compared with the smaller cavity of α -CD.

Here we report the results of MM studies on the complexes of MN with α -CD and β -CD *in vacuo* and in the presence of water, using the Tripos Force Field (50) of

TABLE 1
Bond Lengths, Bond Angles, and Partial Charges in a D-Glucopyranose Unit in •-CD (or •-CD)^a

Bond	Length (Å)	Bonds	Angle (deg)	Atom ^b	Charge (esu)
C1–C2	1.547 (1.547)	O5–C1–C2	109.0 (109.9)	C1	0.327 (0.327)
C2–C3	1.546 (1.544)	C1–C2–C3	109.8 (109.1)	C2	0.096 (0.096)
C3–C4	1.550 (1.554)	C2–C3–C4	110.2 (109.7)	C3	0.098 (0.098)
C4–C5	1.556 (1.558)	C4–C5–C5	109.2 (108.1)	C4	0.121 (0.121)
C5–O5	1.446 (1.444)	C4–C5–O5	111.6 (110.1)	C5	0.144 (0.144)
C1–O5	1.438 (1.437)	C5–O5–C1	114.0 (114.3)	C6	0.167 (0.167)
C2–O2	1.440 (1.440)	C1–C2–O2	109.2 (109.2)	O2	• 0.315 (• 0.315)
C3–O3	1.439 (1.439)	O2–C2–C3	110.4 (110.6)	O3	• 0.330 (• 0.330)
C4–O4	1.449 (1.446)	C2–C3–O2	108.7 (108.0)	O4	• 0.359 (• 0.359)
C5–C6	1.550 (1.551)	O3–C3–C4	110.2 (112.5)	O5	• 0.352 (• 0.352)
C6–O6	1.438 (1.440)	C3–C4–O4	102.7 (105.5)	O6	• 0.317 (• 0.317)
C1–O4'	1.446 (1.442)	O4–C4–C5	114.5 (115.3)		
		C4–C5–C6	111.5 (113.7)		
		C6–C5–O5	106.1 (104.5)		
		C5–C6–O6	110.1 (108.6)		
		O4'–C1–C2	106.8 (109.2)		
		C4–O4–C1'	117.3 (115.6)		
		O4'–C1–O5	113.7 (111.5)		

^a Values for •-CD are in parentheses.

^b Charges for hydrogen atoms (not tabulated) produce a neutral molecule.

Sybyl 6.2 (51). The results are discussed in relationship to the thermodynamic parameters associated with the formation of the complexes and their implications for the driving forces responsible for the process of inclusion.

METHODS

Computational Details

The calculations were performed with Sybyl 6.2 (51) using the Tripos Force Field (50). This force field approximates the conformational energy of a molecule as the sum of terms for bond stretching, angle bending, torsion, van der Waals, electrostatic, and out-of-plane (for aromatic conjugated systems) interactions. A relative permittivity of 3.5 was used for the electrostatic interactions. Use of a value as low as one for the relative permittivity has little effect on the results because electrostatic interactions are not an important source of the stabilization of the complex. The host (CDs) and guest (MN) geometry and charges obtained by AM1 from MOPAC(52) are collected in Tables 1 and 2, respectively. The same charges were used previously for the CDs (36). Extended nonbonded cutoff distances were 8 Å for van der Waals and electrostatic interactions. A few trial calculations using the larger cutoff of 20 Å did not change the total potential energy more than 0.12%. Minimization of the potential energy of the system was performed by the simplex algorithm (53, 54), and conjugate gradient was used as a termination method (54). The termination gradients

were 0.2 and 3.0 for the calculations performed *in vacuo* and in water, respectively. Geometry and charges for water molecules, which were also obtained by MOPAC (52), are a bond length of 0.95 Å, a bond angle of 104.5°, and partial charges of • 0.192 and • 0.394 esu for hydrogen and oxygen atoms, respectively. Aqueous solvation was achieved by using the Molecular Silverware (55) algorithm (MS), which rapidly packs solvent molecules around the solute. The implementation of MS in Sybyl builds a periodic box by adding solvent molecules so that the solvent van der Waals surface does not overlap with the van der Waals surface of the solute. Periodic boundary conditions were employed using a cubic box with sides of 31.62 and 31.87 Å for MN:•-CD and MN:•-CD complexes, respectively.

Starting Conformations

The initial conformation for MN, depicted in Fig. 1, is one of the conformational energy minima where the ester group and the aromatic ring are coplanar, and the torsional angle C–CO–O–CH₃ is in the *trans* state. The initial structures for the CDs were nondistorted, as described previously (36). Following the usual nomenclature, the torsional angles • and • were 0° and • 3°, respectively, and the bond angle at the bridging oxygen atom, •, for the •-1,4 linkages was 130.3° and 121.7° for •-CD and •-CD, respectively. The • dihedral angles were initially in the *trans* conformation. The nondistorted CD torus approximates a truncated cone with bases of radii *R* and *r*, define by the average of the distances

TABLE 2
Bond Lengths, Bond Angles, and Partial Charges in 2-Methyl Naphthoate

Bond	Length (Å)	Bonds	Angle (deg)	Atom ^a	Charge (esu)
C1-C2	1.397	C1-C2-C3	119.9	C1	• 0.106
C2-C3	1.397	C2-C3-C4	119.9	C2	• 0.132
C3-C4	1.397	C3-C4-C10	120.3	C3	• 0.114
C4-C10	1.400	C4-C10-C9	119.7	C4	• 0.128
C10-C5	1.400	C10-C9-C1	119.7	C5	• 0.132
C5-C6	1.400	C9-C1-C1	120.3	C6	• 0.094
C6-C7	1.397	C10-C5-C6	120.3	C7	• 0.109
C7-C8	1.397	C5-C6-C7	119.9	C8	• 0.048
C8-C9	1.397	C6-C7-C8	119.9	C9	• 0.048
C9-C1	1.400	C7-C8-C8	120.3	C10	• 0.011
C9-C10	1.402	C8-C9-C10	119.7	C11	0.330
C7-C11	1.510	C9-C10-C5	119.7	C12	• 0.075
C11-O1	1.230	C1-C9-C8	120.5	O1	• 0.370
C11-O2	1.334	C4-C10-C5	120.5	O2	• 0.227
O2-C12	1.430				

^a Charges for hydrogen atoms (not tabulated) produce a neutral molecule.

from all oxygen atoms of the secondary and primary hydroxy groups, respectively, to the centers C and C' , define by these oxygen atoms. The initial estimates of R and r for \bullet -CD (\bullet -CD) were 3.57 and 3.55 Å (4.31 and 4.34 Å), respectively (36). These values were corrected by subtracting the van der Waals radius of the oxygen atoms (1.36 Å). The depth of the torus, which in both cases is 8.81 Å, was obtained by taking the distance between both centroids C and C' , and corrected by adding twice the van der Waals radius of oxygen. With these parameters, the initial volumes of the cavities were 351 and 518 Å³ for \bullet -CD and \bullet -CD, respectively (36).

Complexation

The origin of a Cartesian coordinate system (denoted by O in Fig. 1) was located at the center of mass of the oxygen atoms of the hydroxyl groups. The y axis of this coordinate system passes through the centroids defined previously as C and C' . It is oriented with the y coordinates of the oxygen atoms in the primary (secondary) hydroxyl groups being negative (positive). It constitutes sixfold and sevenfold rotation axes for the initial conformations of \bullet -CD and \bullet -CD, respectively. The yz plane includes one of the glycosidic oxygen atoms. All glyco-

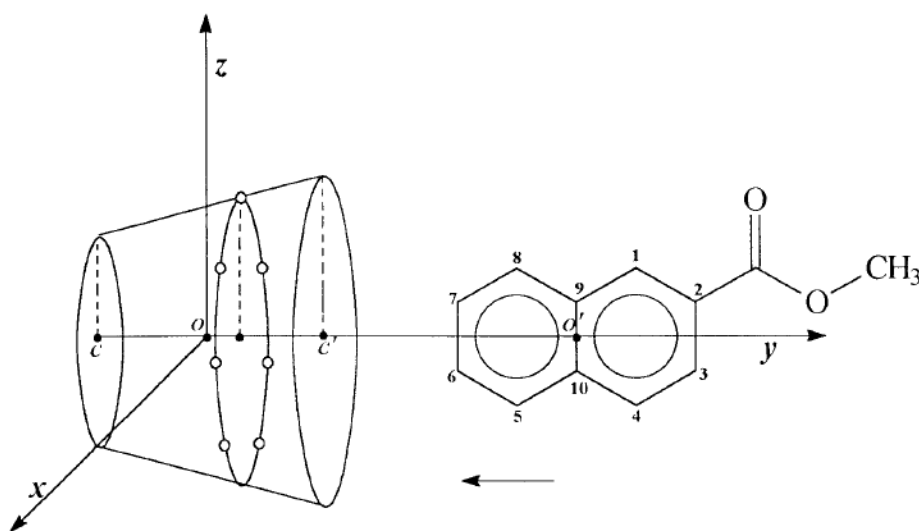


FIG. 1. Coordinate system used to define the process of complexation.

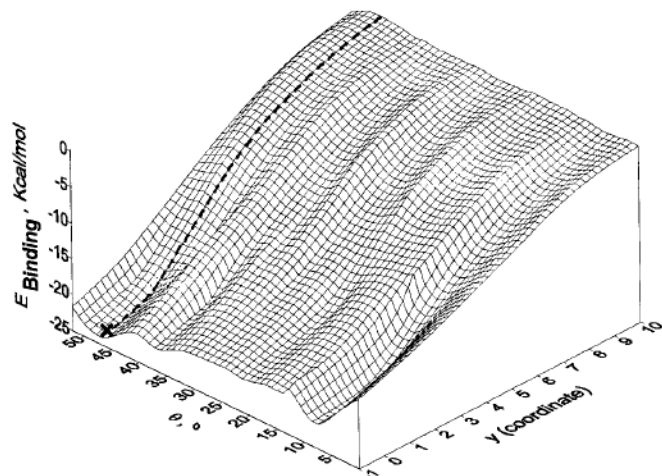
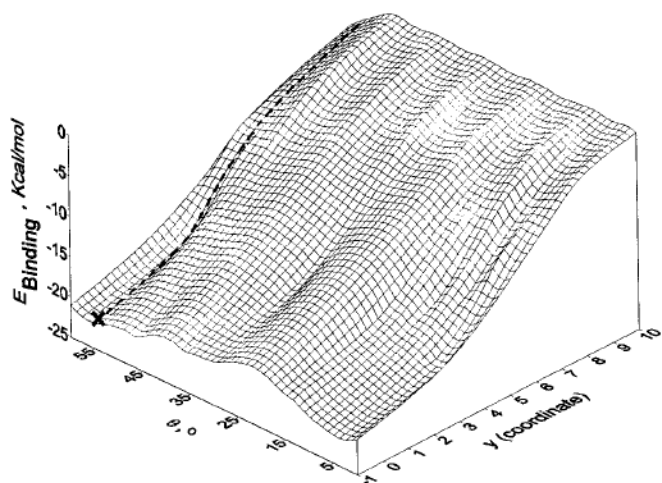


FIG. 2. Three-dimensional plot of E_{binding} versus \bullet and the distance (y , in Å) between the host and guest for (top) A and (bottom) B. The trajectory of lowest energy is highlighted. The y axis is a six(seven)fold rotation axis for A (B).

sic oxygen atoms are placed in a plane nearly parallel to the xz plane, with a y coordinate initially at 0.6 Å. For the complexation process, the host CD was kept in this position while the guest MN approached along the y axis, from the positive direction, so that MN approaches the wider edge of the torus. The y axis and the one that bisects the C2–C3, C6–C7, and C9–C10 bonds of the naphthalene group were colinear during the approach, as shown in Fig. 1. The distance along the y axis, from O to the centroid O' of the C9 and C10 atoms, was used as a measure of the distance between host and guest. The angle \bullet between the yz plane and the plane of the naphthalene ring was used to define the orientation of MN relative to the host. The calculations reported here were performed where the apolar side of the naphthalene (without the ester) approaches the host, as depicted in Fig. 1. The use

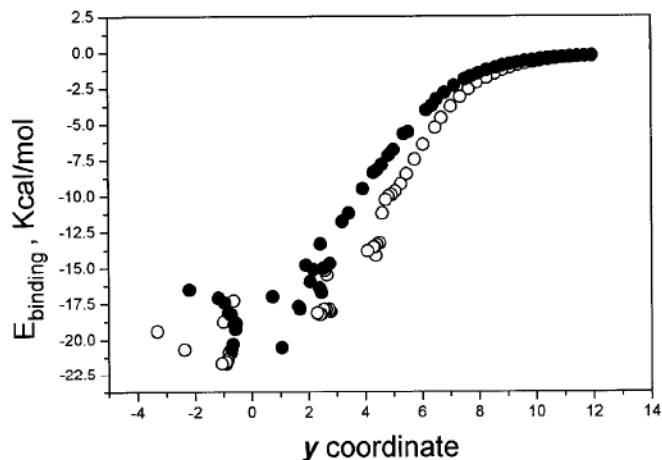


FIG. 3. E_{binding} versus y coordinate (Å) in vacuo for (○) A at $\bullet = 55^\circ$ and (●) B at $\bullet = 46^\circ$.

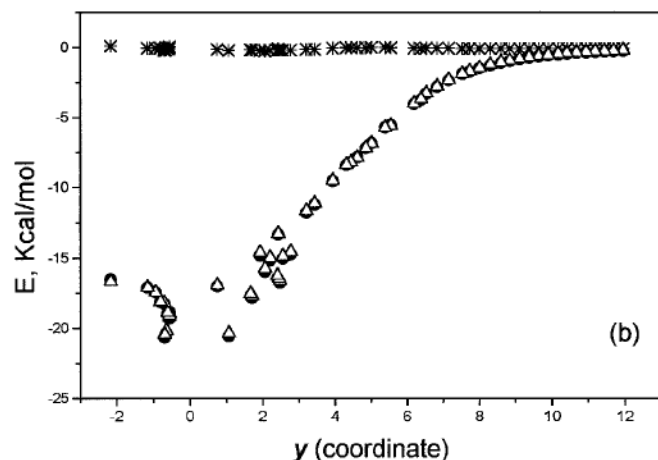
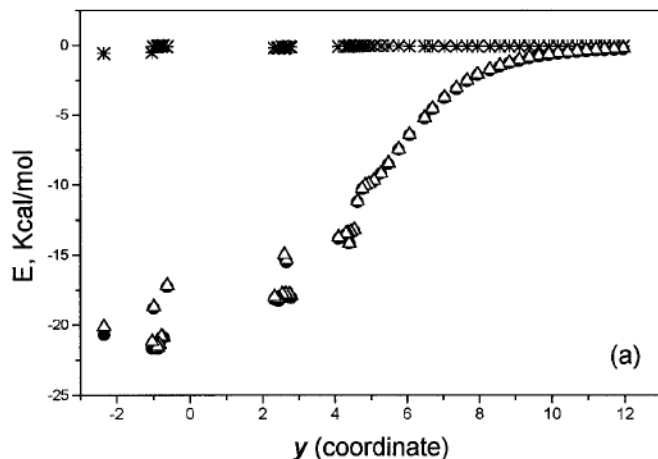


FIG. 4. Van der Waals (Δ) and electrostatic ($*$) contributions to E_{binding} (\bullet), as a function of the y coordinate (Å), for (a) A, using $\bullet = 55^\circ$, and (b) B, using $\bullet = 46^\circ$. The triangles overlay most of the filled circles.

TABLE 3

E_{binding} and Selected Components at the Minimum Energy (Subscript 0) and Infinite Separation of the Two Components (Subscript ∞)

	Energy (kcal/mol)			
	A ₀	A _∞	B ₀	B _∞
E_{binding}	• 21.7	• 0.2	• 20.6	• 0.2
Electrostatic part	• 0.1	• 0.0	• 0.2	• 0.0
Van der Waals part	• 21.6	• 0.2	• 20.4	• 0.2
E_{tot} for MN:CD	83.8	95.6	84.4	110.6
Electrostatic part	48.3	48.8	57.1	56.4
Van der Waals part	• 30.5	• 12.9	• 33.4	• 13.7
E_{tot} for CD	98.6	90.7	99.7	105.6
Electrostatic part	46.8	47.3	56.0	54.9
Van der Waals part	• 11.4	• 15.3	• 15.7	• 16.2
E_{tot} for MN	6.9	5.2	5.3	5.2
Electrostatic part	1.5	1.5	1.5	1.5
Van der Waals part	2.5	2.7	2.7	2.7

of this orientation of MN is supported by observations that unsubstituted naphthalene also forms the complex (56, 57).

The nonbonded interaction between MN and CD, or binding energy, E_{binding} , was obtained as

$$E_{\text{binding}} = E_{\text{MN:CD}} - (E_{\text{isolated MN}} + E_{\text{isolated CD}}). \quad [1]$$

The terms on the right-hand side represent the potential energy of the MN:CD system and the sum of the potential energies of isolated MN and CD in the same conformations. E_{binding} in the presence of water was obtained by removing the water molecules from the box before applying Eq. [1].

The change in the potential energy of the CD on complexation was evaluated as the difference in the potential energy of the CD in the complex and that for the conformation obtained for CD when it is separated from MN by 12 Å (which approximates an infinite separation):

$$E_{\text{CD}} = E_{\text{complexed CD}} - E_{\text{isolated CD}}. \quad [2]$$

The strain energy, E_{strain} , for CD is defined as arising only from the local intramolecular contributions and calculated from the torsional, stretching, and bending energies in Eq. [2].

When calculations were performed in the presence of water as a solvent, a measure of the influence of the solvent on complexation was obtained as the difference between the total potential energy of the entire system $E_{\text{MN:CD} \cdot \text{water}}$ and the sum of the energy of the water molecules E_{water} contained in the solvent box without taking into account the presence of MN and CD and the potential energy of the system

MN:CD by removing the water molecules from the box, $E_{\text{MN:CD}}$:

$$E_{\text{MN:CD} \cdot \text{water}} - E_{\text{MN:CD} \cdot \text{water}} = (E_{\text{MN:CD}} + E_{\text{water}}). \quad [3]$$

RESULTS AND DISCUSSION

Complexation in Vacuo

As in most of the previous investigations (37, 39–48), we initially performed MM simulations of the complexation in the absence of a solvent. The symbols A and B refer to MN:•-CD and MN:•-CD, respectively.

Initially the path was determined for the most favorable approach of MN to the CD. For this purpose, E_{binding} was calculated for all of the optimized structures obtained by scanning ϕ at 10° intervals from 0° to 60° and scanning γ at 1-Å intervals where the separation between CD and MN was 10 to 2 Å. Figure 2 depicts three-dimensional plots of E_{binding} versus ϕ and γ for A and B. E_{binding} passes through

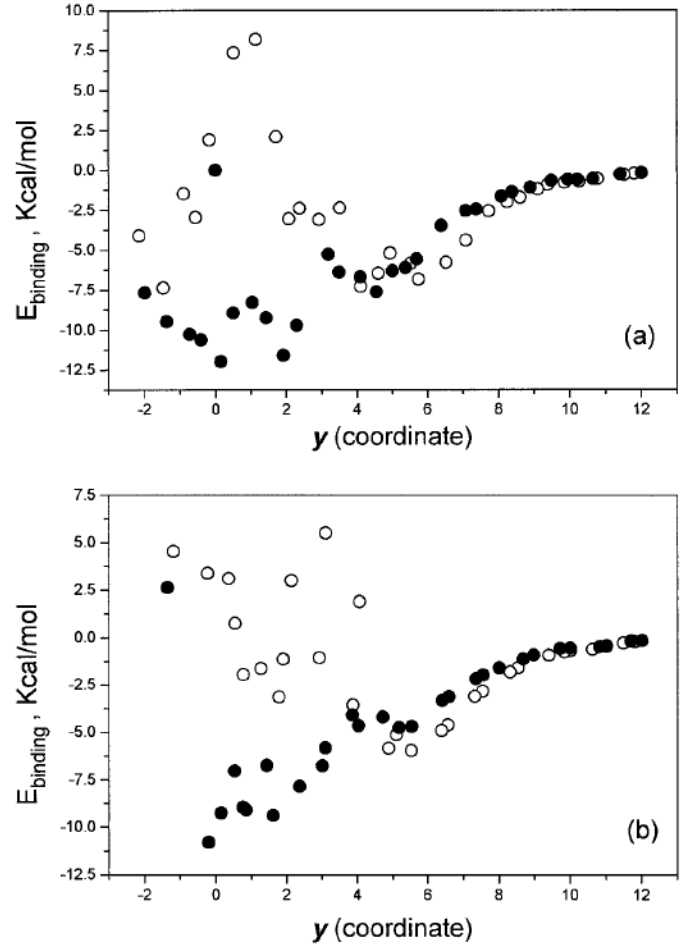


FIG. 5. E_{binding} as a function of the γ coordinate (A) for (○) A (• • 55°) and (•) B (• • 46°) using Method I (a) and Method II (b).

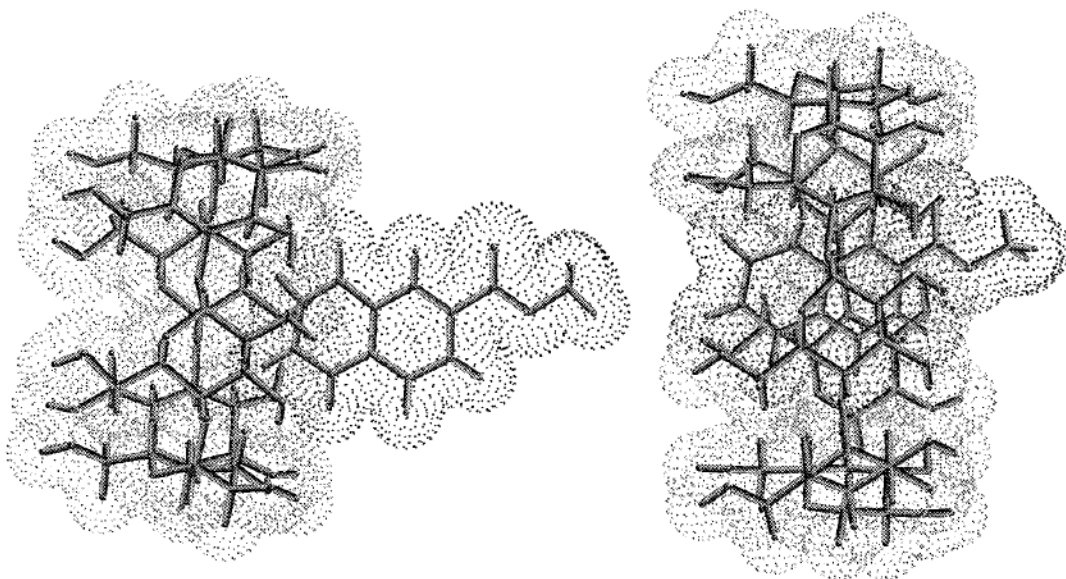


FIG. 6. Van der Waals surfaces for the complexes of (left) A and (right) B. The water molecules are not depicted.

two main minima, which were obtained at approximately $y \cdot \cdot 1 \text{ \AA}$ and $\cdot \cdot 5^\circ$ and 55° ($\cdot \cdot 5^\circ$ and 46°) for A (B), with the minima for 55° and 46° having the more negative E_{binding} . Trajectories of lowest energy for the approach of MN to CD were selected from these three-dimensional plots. In the remainder of this work, results were obtained on the basis of the MN approaching the CD where y is changed from 12 to $\cdot 2 \text{ \AA}$ and \cdot is initially placed at 55° (A) and 46° (B) before optimization.

Figure 3 depicts E_{binding} for A and B for the optimized structures obtained by scanning y from 12 to $\cdot 2 \text{ \AA}$ at 0.25- \AA intervals for the trajectories of minimum energy. The

TABLE 4

E_{binding} and Selected Components at the Minimum Energy (Subscript 0) and Infinite Separation of the Two Components (Subscript ∞) for the Complexes in Water

	Energy (kcal/mol)			
	A ₀	A _{∞}	B ₀	B _{∞}
E_{binding}	$\cdot 5.9$	$\cdot 0.2$	$\cdot 10.8$	$\cdot 0.2$
Electrostatic part	$\cdot 0.1$	0.1	$\cdot 0.3$	$\cdot 0.1$
Van der Waals part	$\cdot 5.9$	$\cdot 0.3$	$\cdot 10.5$	$\cdot 0.2$
E_{tot} for MN:CD	182.9	140.4	236.8	167.5
Electrostatic part	47.0	46.0	55.8	54.5
Van der Waals part	14.2	11.6	$\cdot 2.4$	18.6
E_{tot} for CD	157.4	130.4	218.8	156.8
Electrostatic part	45.4	44.3	54.6	53.0
Van der Waals part	11.4	8.2	3.9	13.3
E_{tot} for MN	31.4	10.3	28.7	10.8
Electrostatic part	1.6	1.6	1.5	1.4
Van der Waals part	8.6	3.6	4.2	5.4

energy of both systems decreases when MN approaches the CD. The most stable structure is reached at approximately $y \cdot \cdot 1 \text{ \AA}$ in both cases. At this point the binding energies are very similar. However, the points on the complexation curve for B are more evenly spaced along y than are the points for A. The gaps for A at approximately $y \cdot 3.5$ and 0.5 \AA are produced by repulsive interactions that are stronger in A than in B. The first repulsion is produced by interaction between hydrogen atoms bonded to C5 and C8 of MN and the C3 axial hydrogen atoms of glucopyranose. The second, wider repulsive region is produced by strong interactions of hydrogen atoms bonded to C5 and C8 (C1 and C4) from MN with hydrogen atoms bonded to C3 (C5) of glucopyranose, respectively. Another difference comes from the value of E_{binding} on complexation. At each y coordinate, the value of E_{binding} for A tends to be slightly more negative than that for B. The variation in entropy on complexation has previously been attributed mainly to changes in solvation or in the degrees of freedom of the system during the process (1–3). Assuming that at large distances (when host and guest begin to interact) these entropic effects could be neglected, E_{binding} will be a measure of the enthalpy, which is slightly more negative for A than for B. Then the values at the minimum of the curves can be correlated with the equilibrium constant for the process.

Figure 4 depicts the van der Waals and electrostatic contributions to E_{binding} during the complexation processes. The van der Waals interactions contribute most of the stabilization of both A and B. From the data collected in lines 7–9 of Table 3, the total potential energy of the CD ring increases slightly for A and decreases slight for B, but never makes the primary contribution to the stabilization of the complexes. A similar

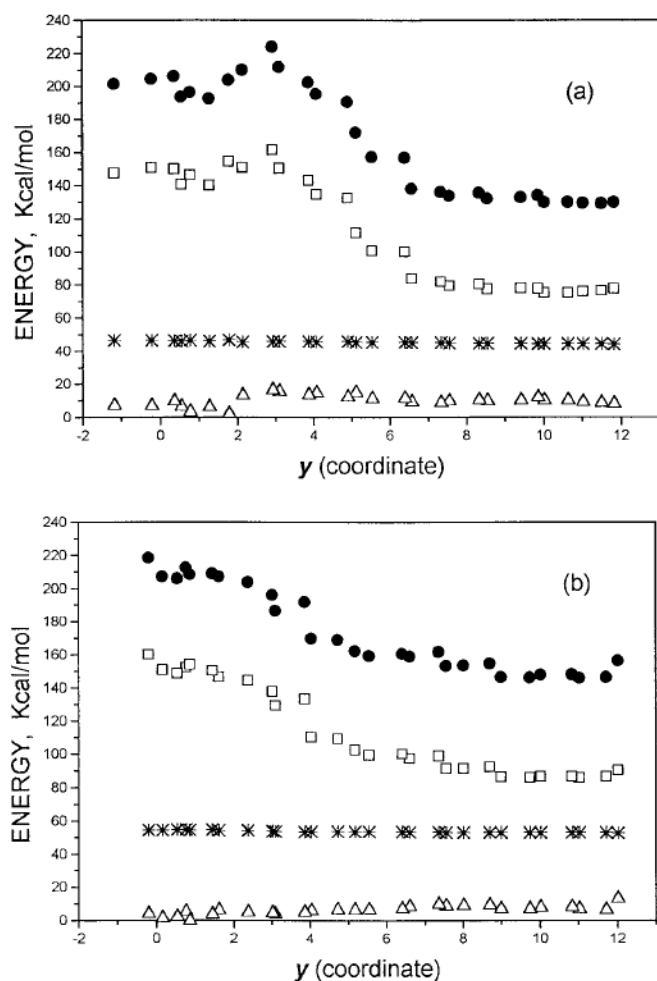


FIG. 7. Energy of the solvated conformation, as a function of y coordinate, for (a) \bullet -CD and (b) \bullet -CD. The energies, obtained with Method II, are (•) total, (Δ) van der Waals, (*) electrostatic, and (\square) sum of stretching, bending, and torsions.

statement applies to the sum of the stretching, bending, and torsional energies of the CD. The formation of **A** requires a slight increase in these three contributions, but formation of **B** is accompanied by a release in strain of the CD ring, achieved by changes for the \bullet and \bullet torsional angles at the bonds to the bridging oxygen atom.

Complexation in the Presence of Water

Solvation was performed using two different applications of the Silverware algorithm (51, 55). Method I is a solvation followed by a minimization of the potential energy of each structure generated by changing the distance between MN and CD. For Method II, the solvation is performed once for the structure generated at $y = 12 \text{ \AA}$, and the energy of the structure is then minimized. The separation (y coordinate) between MN and CD in the hydrated system is then decreased, and the energy of this new system is again minimized, etc.

Figure 5 depicts E_{binding} for **A** and **B** from the optimized structures obtained by scanning y at intervals of 0.5 \AA . Complexation in the presence of water is also thermodynamically favorable. Methods I and II give similar results, but these results differ from those obtained *in vacuo*. In Fig. 5 the most stable structure is reached for both methods at approximately $y = 0 \text{ \AA}$ for **B** and around $y = 5 \text{ \AA}$ for **A**. In the presence of water, the binding energy for **B** is more negative than the binding energy for **A**. Assuming, as previously, that entropic effects are negligible at large MN-CD distances, E_{binding} would be a measure of the enthalpy, which is more negative for **A** than for **B**. These results agree, at least qualitatively, with the experimental stability constants and enthalpies obtained for **A** and **B** complexes by fluorescence measurements (49), which are $\bullet G$ of $\bullet 13.1$ and $\bullet 18.6 \text{ kJ mol}^{-1}$ for **A** and **B**, respectively, and $\bullet H$ of $\bullet 30.9$ and $\bullet 15.1 \text{ kJ mol}^{-1}$ for **A** and **B**, respectively. According to these experimental results, formation of **B** is accompanied by a larger negative free energy change and a smaller negative enthalpy change than formation of **A**.

Since the minimum energy for **B** is obtained near $y = 0 \text{ \AA}$, MN penetrates completely into the cavity. However, for **A** the minimum is obtained at approximately $y = 5 \text{ \AA}$, and MN penetrates only slightly into the cavity. As a result, \bullet -CD is more effective than \bullet -CD in shielding MN from the solvent. Figure 6 depicts the structures of both complexes when their energies have been minimized. The differences in $\bullet S$ for the formation of the two complexes may arise from the difference in the exposure of MN to the solvent, along with the usual entropic effect of the hydrophobic group on the water molecules in its vicinity, as was proposed by Fraiji *et al.* for similar compounds (24).

The nonbonded van der Waals interactions contribute almost all of the stabilization of the complexes formed in water, as was also true for the complexes *in vacuo*. The most important components are summarized in Table 4.

The total potential energy of the CDs, as well as several components, is depicted in Fig. 7. Complexation produces an increase in the energy of the CD, with the increase being larger for **A** than for **B**. The increase in energy is due to a change in the conformation of the CD on formation of the complex. Torsional, bending, and stretching terms contribute most of this increase. There is little contribution from the van der Waals and electrostatic terms.

The energy of the interaction of the solvent with the complexes, denoted by $E_{\text{MN:CD} \cdot \text{water}}$, is depicted in Fig. 8. This hydration energy is strongly negative when the CD and MN are separated by a large distance. As they approach one another, so that the hydration of CD and MN becomes interdependent, the hydration energy becomes less negative. Within the scatter, this energy becomes indistinguishable from zero in the most stable geometries for the complexes.

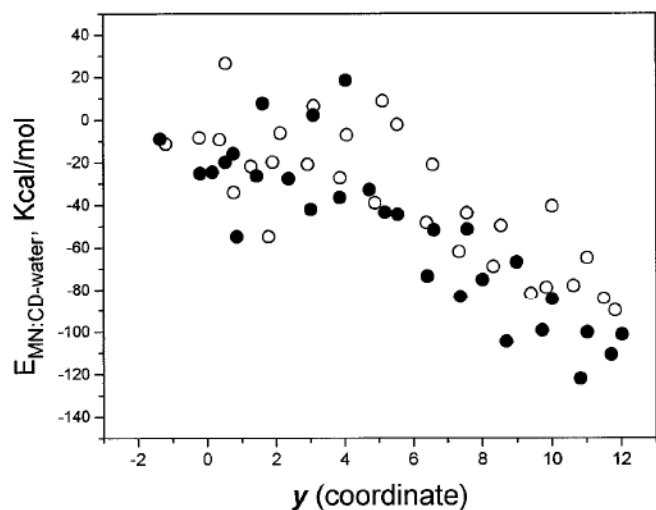


FIG. 8. Interaction energy between the water and the complex for (○) A and (●) B, obtained with Method II.

Therefore the hydration energy serves as a source of destabilization for the complexes.

CONCLUSIONS

MM calculations for the MN:CD systems *in vacuo* and in the presence of water as a solvent reproduce the experimental fact (49) that both 1:1 complexes are thermodynamically stable in water. The nonbonded van der Waals interactions are responsible for this stability, both in water and *in vacuo*. Complexation is accompanied by an increase in strain in the CD macroring. The energy of hydration favors the separation of MN from the CD. The binding energy for the structure of minimum energy is more negative for the formation of B than for the formation of A. This observation in the calculations agrees with the higher stability of B in the experiments. In the complex of minimum energy, MN penetrates completely through the cavity in the •-CD cavity, but it makes only a slight penetration into the cavity of •-CD. This difference in the structures of the two complexes may contribute to the differences in •S for their formation.

ACKNOWLEDGMENTS

This research was supported by CICYT Grant PB94-0364, by the University of Alcalá, (UAH 017/95), and by National Science Foundation Grant DMR 9523278. We express our thanks to Mrs. Heijnen for assistance with the preparation of the manuscript.

REFERENCES

- Bender, M. L., and Komiyama, M., "Cyclodextrins Chemistry." Springer-Verlag, Berlin, 1978.
- Szejtli, J., "Cyclodextrins and Their Inclusion Complexes." Akadémiai Kiadó, Budapest, 1982.
- Szejtli, J., "Cyclodextrins Technology." Kluwer Academic, Dordrecht, 1988.
- Connors, K. A., "Binding Constants: A Measurement of Molecular Complex Stability." Wiley, New York, 1987.
- Matsui, M., and Mochida, K., *Bull. Chem. Soc. Jpn.* **52**, 2808 (1979).
- Yorozu, T., Hoshino, M., Imamura, M., and Shizuka, H., *J. Phys. Chem.* **86**, 4422 (1982).
- Buvari, A., and Szejtli, J., *J. Incl. Phenom.* **1**, 151 (1983).
- Hamai, S., *J. Phys. Chem.* **93**, 2074 (1988).
- Smith, V. K., Ndou, T. T., Muñoz de la Peña, A., and Warner, I. M., *J. Incl. Phenom.* **10**, 471 (1991).
- Mularz, E., Cline-Love, L. J., and Petersheim, M., *Anal. Chem.* **60**, 2751 (1988).
- Harata, K., and Uedaira, H., *Bull. Chem. Soc. Jpn.* **48**, 375 (1975).
- Kobayashi, N., Saito, R., Hino, H., Hino, Y., Ueno, A., and Osa, T., *J. Chem. Soc. Perkin Trans. 2*, 1031 (1983).
- Cromwell, W. C., Byström, K., and Eftink, M. R., *J. Phys. Chem.* **89**, 326 (1985).
- Diard, J. P., Saint-Aman, E., and Serve, D., *J. Electroanal. Chem. Interfacial Electrochem.* **189**, 113 (1985).
- Matsue, T., Osa, T., and Evans, D. H., *Anal. Chem.* **56**, 722 (1981).
- Matsue, T., Fujihara, M., and Osa, T., *J. Incl. Phenom.* **2**, 548 (1984).
- Mohseni, R. M., and Hurtubise, R. J., *J. Chromatogr.* **499**, 395 (1990).
- Fujimura, K., Ueda, T., Masashi, K., Takayanagi, H., and Ando, T., *Anal. Chem.* **58**, 2668 (1986).
- Dong, D. C., and Winnik, M. A., *Photochem. Photobiol.* **35**, 17 (1982).
- Blyshak, L. A., Dobson, K. Y., Patonay, G., Warner, I. M., and May, N. E., *Anal. Chem.* **61**, 955 (1989).
- Agbaria, R. A., Uzan, B., and D. Gill, D., *J. Phys. Chem.* **93**, 3855 (1989).
- Flamigni, L., *J. Phys. Chem.* **97**, 9566 (1993).
- Will, A. Y., Muñoz de la Peña, A., Ndou, T. T., and Warner, I. M., *Appl. Spectrosc.* **47**, 277 (1993).
- Fraiji, E. K., Jr., Cregan, T. R., and Werner, T. C., *Appl. Spectrosc.* **48**, 79 (1994).
- Nakamura, A., Sato, S., Hamasaki, K., Ueno, A., and Toda, F., *J. Phys. Chem.* **99**, 10952 (1995).
- Hamilton, J. A., Steinrauf, L. K., and Van Etten, R. L., *Acta Crystallgr. Sect. B* **24**, 1560 (1968).
- Flohr, K., Patton, R. M., and Kaiser, E. T., *J. Am. Chem. Soc.* **97**, 1209 (1975).
- Kotake, Y., and Janzen, E. G., *J. Am. Chem. Soc.* **111**, 5138 (1989).
- Lipkowitz, K. B., *J. Org. Chem.* **56**, 6357 (1991).
- Linert, W., Margl, P., and Renz, F., *Chem. Phys.* **161**, 327 (1992).
- Dodziuk, H., and Nowinski, K., *J. Mol. Struct. (Theochem.)* **304**, 61 (1994).
- Prabhakaran, M., and Harvey, S. C., *Biopolymers* **26**, 1087 (1987).
- Prabhakaran, M., *Biochem. Biophys. Res. Commun.* **178**, 192 (1990).
- Koehler, J. E. H., Saenger, W., and van Gunsteren, W. F., *J. Mol. Biol.* **203**, 241 (1988).
- Koehler, J. E. H., Saenger, W., and van Gunsteren, W. F., *Eur. Biophys. J.* **16**, 153 (1988).
- Pozuelo, J., Madrid, J. M., Mendicuti, F., and Mattice, W. L., *Comput. Theor. Polym. Sci.* **6**, 125 (1996).
- Harata, K., *Bull. Chem. Soc. Jpn.* **49**, 197 (1976).
- Tabushi, I., Kiyosuke, Y., Sugimoto, T., and Yamamura, K., *J. Am. Chem. Soc.* **100**, 916 (1978).
- Menger, F. M., and Sherrod, J., *J. Am. Chem. Soc.* **110**, 8606 (1988).
- Venanzani, C. A., Canzius, P. M., Zhang, Z., and Bunce, J. D., *J. Comput. Chem.* **10**, 1038 (1989).
- Ohashi, M., Kasatani, K., Shinohara, H., and Sato, H., *J. Am. Chem. Soc.* **112**, 5824 (1990).

42. Jaime, C., Redondo, J., Sánchez, F., Sanchez-Ferrando, F., and Virgili, A., *J. Org. Chem.* **55**, 4772 (1990).
43. Jaime, C., Redondo, J., Sánchez, F., Sanchez-Ferrando, F., and Virgili, A., *J. Mol. Struct.* **248**, 317 (1991).
44. Fotiadu, F., Fathallah, M., and Jaime, C., *J. Incl. Phenom.* **16**, 55 (1993).
45. Fathallah, M., Fotiadu, F., and Jaime, C., *J. Org. Chem.* **59**, 1288 (1994).
46. Ivanov, P. M., and Jaime, C., *Anal. Quim. Int. Ed.* **92**, 13 (1996).
47. Lipkowitz, K. B., Roghothama, S., and Yang, J., *J. Am. Chem. Soc.* **114**, 1554 (1992).
48. Berg, U., Gustavsson, M., and Aström, N., *J. Am. Chem. Soc.* **117**, 2114 (1995).
49. Madrid, J. M., and Mendicuti, F., *Appl. Spectrosc.*, in press.
50. Clark, M., Cramer, R. C., III, and Van Opdenbosch, N., *J. Comput. Chem.* **10**, 982 (1989).
51. Sybyl 6.2, Tripos Associates, St. Louis, Missouri, USA.
52. MOPAC.AM1, included in the Sybyl 6.2 package.
53. Brunel, Y., Faucher, H., Gagnaire, D., and Rasat, A., *Tetrahedron* **31**, 1075 (1975).
54. Press, W. H., Flannery, B. P., Teukolski, S. A., and Vetterling, W. T., "Numerical Recipes: The Art of Scientific Computing," p. 312. Cambridge Univ. Press, 1988.
55. Blanco, M., *J. Comput. Chem.* **12**, 237 (1991).
56. Kano, K., Takenoshita, I., and Ogawa, T., *Chem. Lett. Chem. Soc. Jpn.* 231 (1982).
57. Nelson, G., Patonay, G., and Warner, I. M., *Appl. Spectrosc.* **41**, 1235 (1987).